ISSN- O: 2458 - 868X, ISSN–P: 2458 – 8687
National Library of Medicine - ID: 101731606

International Journal of Medical Science and Innovative Research (IJMSIR)
IJMSIR : A Medical Publication Hub
Available Online at: www.ijmsir.com
Volume – 9, Issue – 5, October – 2024 , Page No. : 148 – 159

Diagnostic Accuracy of MRI in Differentiating Benign from Malignant Bone Tumors Considering Histopathology as Gold Standard

[1]Dr. Bhuvan Maheshwari, Junior Resident, Department of Radiodiagnosis, SNMC, Jodhpur, Rajasthan, India
[2]Dr. Kirti Chaturvedy, Senior Professor and HOD, Department of Radiodiagnosis, SNMC, Jodhpur, Rajasthan, India
[3]Dr. Pradish Sheoran, Assistant Professor, Department of Radiodiagnosis, SNMC, Jodhpur, Rajasthan, India
[4]Dr.Sunil Bishnoi, Assistant Professor, Department of Radiodiagnosis, SNMC, Jodhpur, Rajasthan, India
[5]Dr. Aayush Ajmera, Junior Resident, Department of Radiodiagnosis, SNMC, Jodhpur, Rajasthan, India
Corresponding Author: Dr. Bhuvan Maheshwari, Junior Resident, Department of Radiodiagnosis SNMC, Jodhpur, Rajasthan, India

Citation this Article: Dr. Bhuvan Maheshwari, Dr. Kirti Chaturvedy, Dr. Pradish Sheoran, Dr.Sunil Bishnoi, Dr. Aayush Ajmera, "Diagnostic Accuracy of MRI in Differentiating Benign from Malignant Bone Tumors Considering Histopathology as Gold Standard", IJMSIR - October - 2024, Vol – 9, Issue - 5, P. No. 148 – 159.
Type of Publication: Original Research Article
Conflicts of Interest: Nil

Abstract

Magnetic Resonance Imaging (MRI) remains a crucial modality for diagnosing bone tumors, though its effectiveness in distinguishing benign from malignant lesions continues to be refined. This observational cross-sectional study evaluated the diagnostic capabilities of MRI, focusing on conventional sequences and diffusion-weighted imaging (DWI), with histopathology serving as the definitive reference standard. Conducted at Dr. S.N. Medical College, Jodhpur, the study included 50 patients (28 males and 22 females) presenting with suspected or diagnosed bone tumors. All participants underwent MRI on a 1.5 Tesla Philips Achieva machine, with DWI available in 20 cases due to technical constraints. The highest representation was observed in the 11–20-year age group (36%), with the femur being the most commonly affected site (40%). Benign tumors were dominated by giant cell tumors and aneurysmal bone cysts, while osteosarcoma emerged as the leading malignant diagnosis.

MRI achieved impressive diagnostic accuracy, demonstrating 92.86% sensitivity, 90.91% specificity, and 92% overall accuracy in differentiating benign from malignant tumors. DWI analysis showed that apparent diffusion coefficient (ADC) values were significantly lower in malignant lesions (mean $1.15 \pm 0.564 \times 10^{-3}$ mm^2/s) than in benign tumors (mean $1.75 \pm 0.411 \times 10^{-3}$ mm^2/s), with an optimal threshold of 1.35×10^{-3} mm^2/s for malignancy. Conventional MRI characteristics such as lesion size, margin clarity, periosteal reaction, and contrast enhancement were vital for accurate classification. These results reinforce MRI's diagnostic utility in characterizing bone tumors, with particular advantages noted for younger populations. While DWI demonstrates substantial potential, a larger sample size is recommended to establish more robust quantitative benchmarks. This study supports MRI's role as a

valuable diagnostic tool in assessing and managing bone tumors.

Keywords: MRI, Bone Tumors, Benign, Malignant, Histopathology, Diagnostic Accuracy, Diffusion-Weighted Imaging (DWI), Apparent Diffusion Coefficient (ADC)

Introduction

Bone lesions and tumors pose a significant diagnostic challenge, often necessitating a variety of imaging modalities for accurate assessment. Although conventional radiography remains the initial imaging choice, MRI has proven invaluable as an adjunct, especially for lesions exhibiting aggressive characteristics [(1).] Its high contrast resolution and multiplanar imaging capabilities make MRI particularly effective for evaluating both the intra- and extra-compartmental spread of tumors, offering critical insights into surrounding structures like perilesional muscles, neurovascular bundles, and fat planes [(2).]

Advanced 3 Tesla MRI technology, with its enhanced signal-to-noise ratio and superior spatial resolution, has notably improved diagnostic accuracy [(3).] Techniques like contrast-enhanced MRI and diffusion-weighted imaging further expand MRI's utility, allowing more precise biopsy guidance by helping avoid necrotic areas [(4,5).] While MRI is highly sensitive for distinguishing between benign and malignant lesions based on bone marrow changes, its specificity can vary due to the diverse presentations of lesions on T1 and T2-weighted sequences [(6,7,8).]

Despite these advancements, histopathological confirmation remains essential for a definitive bone tumor diagnosis [(9).] MRI continues to play an expanding role in surgical planning, treatment monitoring, and post-therapy assessments [(10).] Thus, this study aims to evaluate MRI's diagnostic accuracy in distinguishing benign from malignant bone tumors, considering histopathology as the gold standard [(11,12).]

The primary objectives include assessing MRI's sensitivity, specificity, and predictive values for differentiating benign from malignant tumors, and identifying imaging features that aid in this differentiation. This comprehensive analysis is intended to establish MRI's reliability in characterizing bone tumors, ultimately aiding clinicians in informed decision-making for patient management.

Materials and methods

Study Design and Population

An observational cross-sectional study was conducted in the Department of Radio-diagnosis at Dr. S.N. Medical College, Jodhpur, and associated hospitals. The study included patients of all age groups with clinically suspected or diagnosed primary bone tumors who consented to undergo MRI followed by histopathological examination. Patients with contraindications for MRI (metallic implants, cardiac pacemakers, metallic foreign bodies, claustrophobia) and those with poor image quality or artifacts were excluded. The sample size of 50 subjects was calculated based on expected sensitivity of 94% and specificity of 90% at 95% confidence interval with a relative precision of 15%.

MRI Protocol and Image Acquisition

All imaging was performed using a 1.5 Tesla Philips Achieva Machine with appropriate body/surface coils. The standard protocol included T1-weighted images (coronal and sagittal), T2-weighted images (axial and sagittal), STIR/PDFS sequences (sagittal and coronal), and post-contrast fat-saturated T1W images. Large field of view T1/STIR images were obtained to identify skip lesions. Diffusion-weighted imaging (DWI) was performed in 20 patients using b-values of 0, 500, and 1000 s/mm² with ADC map generation. Slice thickness

was maintained at 4-5 mm, and contrast-enhanced images were obtained after intravenous gadolinium administration.

Image Analysis

Two experienced radiologists, blinded to clinical and other radiological information, independently analyzed the MR images, with discrepancies resolved by a third radiologist. The analysis included:

- Lesion location and intramedullary extent
- Signal characteristics relative to adjacent muscle
- Margin definition (well-defined or ill-defined)
- Enhancement patterns (homogeneous, heterogeneous, or absent)
- Presence of skip lesions, cortical involvement, and soft tissue components
- Joint and neurovascular involvement
- ADC values in cases with DWI

Diagnostic criteria for benign lesions included well-defined margins, lobulated shape, small size, absence of periosteal reaction, neurovascular involvement, and soft tissue component. Malignant features included large size, periosteal reaction, cortical destruction, neurovascular involvement, soft tissue component, enhanced post-contrast studies, and bone marrow involvement.

Statistical Analysis

The diagnostic accuracy was evaluated by calculating sensitivity, specificity, positive predictive value, and negative predictive value. Categorical variables were expressed as numbers and percentages and analyzed using Chi-square test, while continuous variables were expressed as mean and standard deviation and analyzed using T-test. Interobserver variability was assessed using Cohen's kappa statistic. SPSS software was used for all statistical analyses.

All imaging findings were correlated with histopathological examination results, which served as the gold standard for final diagnosis. The study was conducted after obtaining institutional ethical committee clearance, and informed consent was obtained from all participants.

Result & Discussion

This study analyzed 50 patients with primary bone tumors using both MRI and histopathological examination (HPE), with the aim of evaluating MRI's diagnostic accuracy in differentiating benign from malignant tumors. MRI, as a non-invasive imaging modality, provides valuable insights into tumor characteristics such as size, signal intensity, tissue involvement, and the presence of aggressive features, which are crucial for diagnostic accuracy and treatment planning. Below, the results are discussed with a comprehensive interpretation of their clinical significance, along with a comparison to existing literature.

Demographic Distribution and Pathology

The patient cohort in this study had a higher incidence of primary bone tumors in the 11-20 year age group (36%), with males being more commonly affected than females (56% vs. 44%). This aligns with the findings of Obalum et al., where the peak age for primary bone tumors was similarly in the 11-20 year range, with a male-to-female ratio of 1.5:1[13]. He XH et al. also reported a predominance of tumors in individuals aged 11-40[14]. This demographic data reflects the typical age and sex distribution of primary bone tumors, which often affect adolescents and young adults, particularly males. In terms of pathology, benign tumors accounted for 44% of cases, while malignant tumors were slightly more prevalent (56%). Among the benign tumors, Giant Cell Tumor (GCT) and Aneurysmal Bone Cyst (ABC) were

the most common, each representing 10% of cases. The most frequently observed malignant tumors were Osteosarcoma (24%) and Ewing's Sarcoma (10%). These findings are consistent with the literature, where osteosarcoma is widely regarded as the most common primary bone malignancy [13,14].

Skeletal and Bone Involvement

In this study, 68% of tumors were located in the appendicular skeleton, while the remaining 32% involved the axial skeleton. The femur was the most frequently affected bone (40% of cases), followed by the humerus (18%) and the spine (14%). The predominance of femur involvement aligns with previous studies, which indicate that the long bones, particularly the femur, are the most common sites for both benign and malignant bone tumors.

Tumor Size as a Predictor of Malignancy

The size of the tumors was a significant predictor of malignancy in this study. Tumors larger than 6 cm were exclusively malignant (n=19), while tumors smaller than 6 cm were predominantly benign (71%). This strong correlation between tumor size and malignancy aligns with Lodwick et al., who noted that larger tumors are more likely to be aggressive and malignant[15]. MRI's ability to accurately measure tumor size and assess its relationship with adjacent structures is crucial in determining the nature of the lesion and guiding treatment decisions.

Periosteal Reaction: A Key Feature in Malignant Tumors

MRI identified periosteal reactions in 80% of cases, with 91% of these reactions being associated with malignant tumors. This finding highlights the importance of periosteal reaction as a marker of malignancy. Murphy et al. described aggressive periosteal reactions, such as Codman's triangle or sunburst patterns, as characteristic features of osteosarcoma and other aggressive bone tumors[16]. In our study, periosteal reaction was also noted in benign cases, although it was less common and usually less aggressive in appearance. The ability of MRI to detect subtle periosteal changes, even when radiographs fail to reveal them, underscores its value in early diagnosis and treatment planning.

Cortical Disruptions and Soft Tissue Extension: Markers of Tumor Aggressiveness

Cortical breaks were detected in 56% of malignant cases, with MRI showing greater sensitivity for identifying these breaks compared to radiographic imaging. Soft tissue invasion, a key indicator of aggressive tumor behavior, was found in 48% of cases, primarily in malignancies. These findings underscore MRI's vital role in evaluating both cortical disruption and soft tissue extension, which are crucial for surgical planning. Previous research by Boyko et al. and others has demonstrated MRI's advantage in distinguishing soft tissue extension and cortical breaks with high accuracy [17].

Neurovascular and Joint Involvement

Neurovascular involvement was observed in 16% of cases, all of which were malignant. MRI's capability to visualize neurovascular structures and assess their relationship to the tumor provides essential information for determining surgical resectability and planning limb-sparing procedures. Jelinek et al. have highlighted the importance of MRI in evaluating neurovascular involvement, a factor that directly influences prognosis and surgical planning [18]. Joint involvement was noted in 20% of cases, all malignant, particularly in osteosarcoma, Ewing's sarcoma, and chondrosarcoma. MRI's effectiveness in assessing articular cartilage invasion or synovial extension is especially valuable in these cases, where joint invasion complicates surgical management.

Diffusion-Weighted Imaging (DWI) and Apparent Diffusion Coefficient (ADC)

DWI and ADC values have shown significant utility in distinguishing benign from malignant lesions. In our study, diffusion restriction was present in 8 cases—all malignant—while 12 cases showed no restriction, with only 2 being malignant. Malignant lesions had a mean ADC of 1.15 ± 0.564 x 10^{-3} mm^2/s, notably lower than benign lesions, which averaged 1.75 ± 0.411 x 10^{-3} mm^2/s. An ADC threshold of 1.35 x 10^{-3} mm^2/s was identified as optimal. These findings align with those of Wang et al. and Pekcevik et al., who reported similar ADC cutoffs for differentiating benign from malignant tumors [19, 20]. Interestingly, chondrosarcoma had the highest ADC values among malignant tumors (2.1 x 10^{-3} mm^2/s), whereas Ewing's sarcoma exhibited the lowest (0.56 ± 0.058 x 10^{-3} mm^2/s), reflecting the distinct cellular density and water diffusion characteristics of different tumor types.

Enhancement Patterns on MRI

In this study, contrast-enhanced MRI identified enhancement in 32 cases, of which 27 were malignant. Conversely, 18 cases showed no enhancement, with 17 of these being benign. Malignant tumors displayed heterogeneous enhancement, indicative of increased vascularity and neovascularization associated with aggressive behavior. This observation is consistent with findings from Pekcevik et al., who emphasized the diagnostic value of enhancement patterns in differentiating benign from malignant bone tumors [20].

Pathological Fractures and Skip Lesions

Pathological fractures were detected by MRI in 6 cases, evenly distributed between benign and malignant lesions, highlighting MRI's utility in treatment planning, as these fractures can impact surgical approaches. Skip lesions, found in 2 cases of osteosarcoma, represent separate tumor foci and are important for prognosis and surgical strategy. MRI's ability to detect skip lesions, which may be overlooked by other modalities, is particularly valuable, as noted by Shimose et al. [21].

Concordance between MRI and Histopathology

The concordance between MRI and histopathological findings in this study was 92%, with MRI showing a sensitivity of 92.88% and specificity of 90.91%. These results align with prior studies, such as those by Yeshlawath et al. and Farooq A et al., which reported MRI sensitivity ranging from 94% to 100% [22, 23]. There were, however, 4 misdiagnosed cases (8%), where MRI incorrectly identified benign lesions as malignant and vice versa. Notably, two cases of osteomyelitis were mistaken for Ewing's sarcoma, reflecting the diagnostic challenges in differentiating infections from malignancy on MRI, a difficulty also reported by McCarville et al. [24]. Additionally, two low-grade chondrosarcomas were misclassified as benign, underscoring MRI's limitations in accurately identifying low-grade malignancies.

Diagnostic Performance of MRI

MRI demonstrated a sensitivity of 92.88%, specificity of 90.91%, and an overall accuracy of 92% in distinguishing between benign and malignant bone tumors. These findings, supported by Bhuyan et al., highlight MRI's critical role in the diagnostic evaluation of primary bone tumors [25]. MRI's ability to provide multiplanar images and superior contrast of soft tissues makes it invaluable for assessing tumor size, aggressiveness, and extent, informing both diagnostic and therapeutic decisions.

Limitations of MRI

Despite its high diagnostic performance, MRI has limitations, particularly in differentiating low-grade malignant tumors from benign lesions. In this study, two low-grade chondrosarcomas were misclassified as

benign, a common challenge in imaging [26]. Additionally, distinguishing between certain benign inflammatory conditions, such as osteomyelitis, and malignant tumors can be difficult, as evidenced by the misclassification of two osteomyelitis cases in this study.

Figures & Tables

Table 1: Comparison of MRI and Histopathological Diagnoses

Diagnosis	MRI Count	HPE Count	Concordant Cases	Discrepancies
Benign Tumors				
Giant Cell tumor	5	5	5	-
Aneurysmal bone cyst	5	5	5	-
Unicameral bone cyst	2	2	2	
Osteochondroma	2	2	2	
Osteoid osteoma	3	3	3	
Chondroblastoma	3	2	2	1 diagnosed as Clear cell chondrosarcoma on HPE
Enchondroma	2	1	1	1 diagnosed as Low-grade chondrosarcoma on HPE
Osteomyelitis	0	2	0	
Malignant Tumors				
Osteosarcoma	12	12	12	
Ewing's sarcoma	7	5	5	2 misdiagnosed, actually osteomyelitis
Chondrosarcoma	2	4	2	2 additional cases (misdiagnosed as benign on MRI)
Plasmacytoma	2	2	2	
Metastasis	5	5	5	
Total	50	50	46	4 discrepancies

Interpretation

- Overall concordance: 46 out of 50 cases (92%) were correctly diagnosed by MRI.
- Misdiagnoses: 4 cases (8%) were misclassified by MRI.
- Nature of discrepancies:

➢ 2 benign lesions (osteomyelitis) were misdiagnosed as malignant (Ewing's sarcoma)

➢ 2 low-grade malignant lesions were misdiagnosed as benign

Figure 1: Distribution of based on specific diagnosis on MRI and number of cases

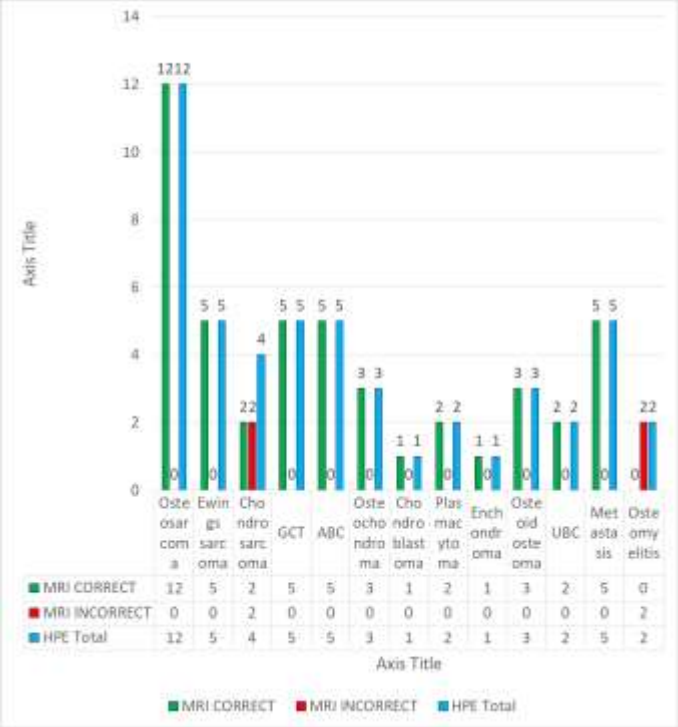

Table 2: Mean ADC levels comparison between malignant and benign lesions

ADC	Benign on HPE		Malignant on HPE	
	MEAN	SD	MEAN	SD
	1.75	0.411	1.15	0.564

ADC, apparent diffusion coefficient; HPE, histopathological examination. χ 2 = 1.020, df = 2, p = 0.02*

The mean ADC in malignant lesions was 1.15± 0.564 and in benign lesions was 1.75 ± 0.411. This difference in mean ADC levels between malignant and benign lesions was statistically significant

Figure 2: Box Plot of ADC Values for Benign and Malignant Tumors

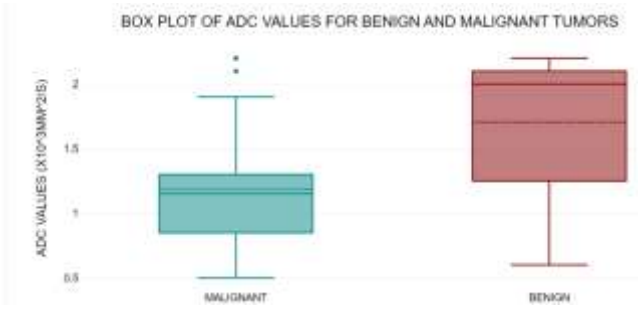

The box plot displays the distribution of ADC values between benign and malignant tumors.

- Median ADC Values: Malignant tumors show a lower median ADC value compared to benign tumors. The median for malignant tumors appears to be around 1.15 x 10^{-3} mm2/s, while for benign tumors it's approximately 1.75x 10^{-3} mm2/s.
- Range of ADC Values:
  - Malignant tumors: Approximately 0.6 to 2.2 x 10^{-3} mm2/s
  - Benign tumors: Approximately 1.2 to 2.2 x 10^{-3} mm2/s
  - General Trend: Overall, lower ADC values tend to be associated with malignant tumors, while higher ADC values are more characteristic of benign tumors.

Table 3: ROC curve showing ADC cut-off for benign and malignant lesions

Area under the curve			
Test result Variable(s): ADC			
Area	SE	p-value	Asymptotic 95% confidence interval
			Lower bound
0.808	0.062	<0.001*	0.686

ADC cut-off	Sensitivity	Specificity
0.55	1.000	0.045
0.85	0.897	0.318
1.35	0.759	0.773
2.15	0.138	0.955

ADC, apparent diffusion coefficient; ROC, receiver operating characteristic; SE, standard error. Notes:

1. The area under the curve (0.808) indicates good discriminatory ability.

2. The p-value (<0.001) suggests that the test is statistically significant.
3. The optimal cut-off of 1.35 x 10^{-3} mm2/s provides the best balance between sensitivity and specificity.
4. Lower ADC cut-offs increase sensitivity but decrease specificity, while higher cut-offs do the opposite.
5. Using this cutoff, you can correctly identify about 76% of malignant lesions (sensitivity) and 77% of benign lesions (specificity).
6. The overall accuracy of 76.5% indicates that this cutoff will correctly classify about 3 out of 4 lesions.

Figure 3: ROC curve showing ADC cut-off for benign and malignant lesions

Figure 4: Scatter plot of ADC values for individual tumors

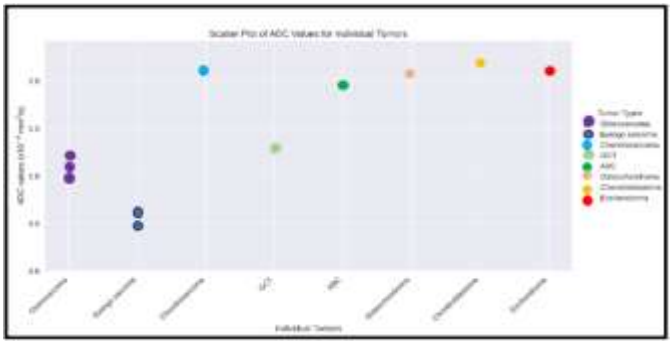

Key observations

1. Osteosarcoma has multiple data points clustered around 1.0-1.2 x10^{-3} mm2/s.
2. Ewing's sarcoma shows the lowest ADC values, around 0.5-0.6 x10^{-3} mm2/s.
3. Chondrosarcoma, Osteochondroma, Chondroblastoma, and Enchondroma have the highest ADC values, all above 2.0 x10^{-3} mm2/s.
4. GCT (Giant Cell Tumor) has tightly clustered values around 1.26-1.27 x10^{-3} mm2/s.
5. ABC (Aneurysmal Bone Cyst) has values just below 2.0 x10^{-3} mm2/s.

Table 4: Showing comparison of benign and malignant tumors

Tumor Characteristics		Benign Tumors	Malignant Tumors
Size <6cm		22	9
Size >6 cm		0	19
Well defined Margins		20	1
Ill Defined Margins		2	27
Wide Zone of transition		2	26
Narrow zone of transition		20	2
Aggressive Periosteal reaction		2	21
Cortical Breach		6	22
Neurovascular bundle involvement		0	8
Enhancement No Heterogenous Homogenous		 17 2 3	 1 27 0
Soft tissue involvement		7	17
Joint Involvement		0	10
*Diffusion restriction	Present Absent	0 10	8 2
Pathological Fracture		3	3
Skip lesions		0	2

*DWI was carried out in 20 cases only.

Table 5: Multivariate Logistic Regression Analysis of MRI Features Predicting Malignancy

MRI Feature	Odds Ratio	95% CI	p-value
Size > 6cm	3.18	1.66-6.09	0.004
Ill-defined margins	5.39	2.81-10.33	<0.001
Wide zone of transition	4.92	1.45 - 16.67	0.010
Aggressive periosteal reaction	3.76	1.12 - 12.63	0.032
Cortical Involvement/ breach	2.58	1.29-5.16	0.007
Soft tissue involvement	2.00	1.00-4.00	0.050
Heterogeneous enhancement	4.75	2.37-9.50	<0.001
Neurovascular bundle involvement	7.24	3.62-14.48	<0.001
Skip lesions	5.86	2.93-11.72	<0.001
Diffusion restriction	5.41	1.62 - 18.06	0.006
ADC value < 1.35 x 10-3 mm2/s	6.08	3.04-12.16	<0.001

The multivariate logistic regression analysis reveals several MRI features as significant predictors of malignancy in bone tumors. Neurovascular bundle involvement emerged as the strongest predictor (OR: 7.24, 95% CI: 3.62-14.48, $p<0.001$), followed closely by ADC values $\leq 1.35 \times 10^{-3}$ mm²/s (OR: 6.08, 95% CI: 3.04-12.16, $p<0.001$) and the presence of skip lesions (OR: 5.86, 95% CI: 2.93-11.72, $p<0.001$). Other significant predictors include ill-defined margins, heterogeneous enhancement, and wide zone of transition, all with odds ratios above 4.0 ($p<0.001$ for each).

These findings suggest that tumors involving neurovascular bundles, exhibiting restricted diffusion (low ADC values), or presenting with skip lesions are substantially more likely to be malignant. The presence of ill-defined margins and heterogeneous enhancement also strongly indicate malignancy. While all examined features showed statistical significance, soft tissue involvement demonstrated the weakest association (OR: 2.00, 95% CI: 1.00-4.00, p=0.050).

Figure 5: Forest plot illustrating the odds ratios and their 95% confidence intervals for MRI features predicting malignancy.

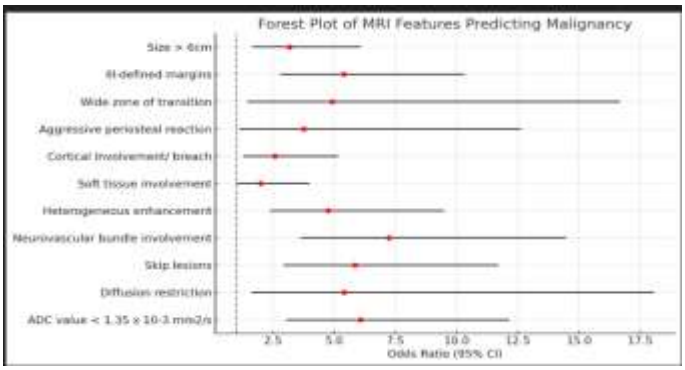

The vertical blue dashed line at x=1 serves as a reference. Features with odds ratios significantly greater than 1 indicate a higher likelihood of malignancy.

This forest plot shows that MRI features such as ill-defined margins, neurovascular bundle involvement, and low ADC values have strong associations with predicting malignancy in primary bone tumors, with significant odds ratios and confidence intervals indicating their diagnostic value.

Table 6: Diagnostic variables of MR imaging

Diagnostic variables of MR imaging	MRI
Sensitivity TP/(TP+FN)	92.88%
Specificity TN/(TN+FP)	90.91%
Positive predictive value TP/(TP+FP)	92.88%

Negative predictive value TN/(TN+FN)	90.91%
Diagnostic Accuracy (TP+TN)/All Patients	92%

The association of MRI diagnosis and histopathological diagnosis was carried out by using Chi-square test, which showed statistical significance with $p<0.04$ in table 6. Study showed sensitivity, specificity and accuracy in differentiating benign from malignant as 92.86%, 90.91% and 92%

Figure 6: Biopsy proven case of Osteosarcoma

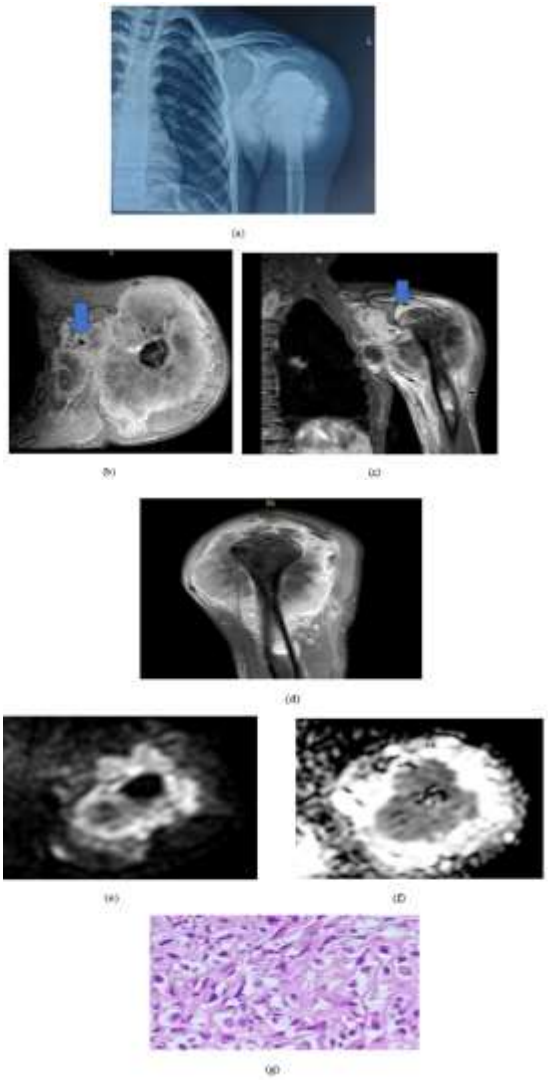

Figure 6 (a to g) A 18 year old male presented with pain and swelling of left shoulder . (a)AP view of Xray left shoulder shows an aggressive expansile lytic sclerotic lesion with sunburst periosteal reaction , wide zone of transition and soft tissue extension noted in proximal meta-diaphysis of left humerus (b)Axial PDFS (c)STIR Coronal (d) T1 Post contrast sagittal (e)DWI (f)ADC shows A destructive STIR hyperintense lesion with periosteal elevation and heterogenous T1 post contrast enhancement and diffusion restriction (ADC value: $1.0x10^{-3}$ mm2/s).with soft tissue extension noted in proximal meta-diaphysis of left humerus , In figure (b) blue arrow shows the lesion shows encasement of neurovascular bundle in axillary pouch . Figure (c) blue arrow shows intra-articular extension of tumor . (g) H&E stained slide shows sheets of cells with atypia and mitoses with areas of atypical osteoid and few giant cells – s/o Osteosarcoma

Figure 7: Biopsy proven case of Ewings sarcoma

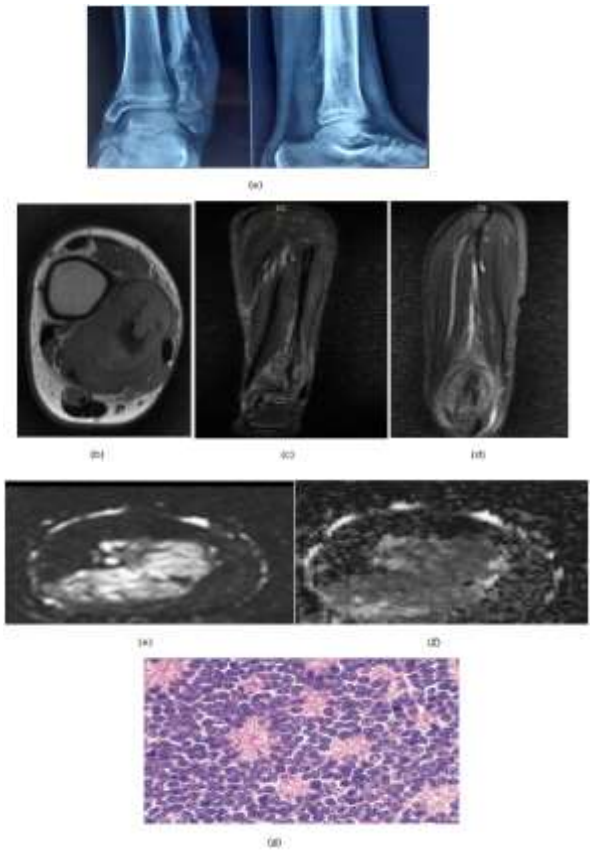

Figure 7 A 10 year old female presented with fever , pain and swelling in distal left leg . (a) AP and lateral radiography of left lower leg shows an ill defined

aggressive permeative lytic lesion with interrupted periosteal reaction and wide zone of transition noted in distal diaphysis of left fibula . (b) Axial T2 (c) Coronal T2 STIR (d) Sagittal STIR (e) DWI (f) ADC An ill defined T2 / STIR hyperintense permeative lesion with periosteal reaction and soft tissue extension showing diffusion restriction in the form of hyperintensity on DWI and hypo-intensity on ADC (mean ADC value 0.7) .(g) High power view showing sheets of small round blue cells with prominent nuclei and minimal cytoplasm forming pseudo rosettes-s/o Ewings sarcoma

Conclusion

MRI demonstrates high diagnostic accuracy in differentiating benign from malignant bone tumors, particularly in the most commonly affected young population and frequently involved bones like the femur. Although the integration of DWI and ADC values significantly enhances its diagnostic capability, the limited number of DWI cases due to technical issues suggests the need for further studies. These findings support the use of MRI as a primary imaging modality for comprehensive assessment and management of bone tumors across various presentations.

References

1. Bestic JM, Wessell DE, Walker EA, Ying-Kou Yung E, Kransdorf JM, ACR Appropriateness Criteria. Primary Bone Tumors. J Am College Radiol 2013; 17(5): s226-38.
2. Baweja S, Arora R, Singh S, Sharma A, Narang P, Ghuman S, et al. Evaluation of bone tumors with magnetic resonance imaging and correlation with surgical and gross pathological findings. Ind J RadiolIm 2008; 16(4): 611-18.
3. Wong S, Steinbach L, Zhao J, Benjamin CS, Link TM. Comparative study of imaging at 3.0 T versus 1.5 T of the knee. Skeletal Radiol 2009; 38(8): 761–69.
4. Ojala R, Sequeiros RB, Klemola R, Vahala E, Jyrkinen L, Tervonen O. MR-guided bone biopsy: preliminary report of a new guiding method. J Magn Reson Imaging 2002; 15(1): 82–86.
5. Poulsen MH, Petersen H, Hoilund-Carlsen PF, Jakobsen JS, Gerke O, Karstoft J, et al. Spine metastases in prostate cancer: comparison of technetium-99m-MDP whole-body bone scintigraphy, [(18) F]choline positron emission tomography (PET)/ computed tomography (CT) and [(18) F]NaF PET/CT. BJU Int 2014; 114(6): 818-23.
6. Palmedo H, Marx C, Ebert A, Kreft B, Ko Y, Turler A, et al. Whole-body SPECT/CT for bone scintigraphy: diagnostic value and effect on patient management in oncological patients. Eur J Nucl Med Mol Imaging 2014; 41(1): 59-67.
7. Wang T, Wu X, Cui Y, Chu C, Ren G, Li W. Role of apparent diffusion coefficients with diffusion weighted magnetic resonance imaging in differentiating between benign and malignant bone tumors. World J Surg Oncol 2014; 12(1): 365-70.
8. Albano D, Patti C, Lagalla R, Midiri M, Galia M. Whole-body MRI, FDG-PET/CT, and bone marrow biopsy, for the assessment of bone marrow involvement in patients with newly diagnosed
9. Lange MB, Nielsen ML, Andersen JD, Lilholt HJ, Vyberg M, Petersen L. Diagnostic accuracy of imaging methods for the diagnosis of skeletal malignancies: A retrospective analysis against a pathology-proven reference. Eur J Radiol 2016; 85(1): 61-67
10. Douis H, Jeys L, Grimer R, Vaiyapuri S, Davies AM. Is there a role for diffusion-weighted MRI (DWI) in

the diagnosis of central cartilage tumors?. Skeletal Radiol 2015; 44(7): 963–69.

11. Wolfgang Schima, Gabriele Amann. Preoperative Staging of Osteosarcoma: Efficacy of MR imaging in detecting joint involvement. AJR 1994 ;163 .1171-1175.
12. Balzarini L, Sicilia A, Ceglia E, Tesoro Tess JD, Trecate G, Musumeci R. Magnetic resonance in primary bone tumors: a review of 10 years of activities. Radiol Med. 1996 Apr; 91(4):344-7
13. Obalum DC, Giwa SO, Banjo AF, Akinsulire AT. Primary bone tumours in a tertiary hospital in Nigeria: 25 year review. Niger J Clin Pract. 2009 Jun;12(2):169-72. PMID: 19764668.
14. He XH. Analysis of 1355 cases of tumours and tumour-like lesions of bone. Zhonghua-Zhong Liu Za Zhi.1990; 12(l):66-8.
15. Lodwick GS. A probabilistic approach to the diagnosis of bone tumors. Radiol Clin North Am. 1965;3:487–497. PMid:5846856.
[PubMed] [Google Scholar]
16. Murphy, Mark Robbin, Gina Mcrae, D Hemming, T Temple, M kransdorf. The many faces of osteosarcoma. Radiographics 1997; 17: 1205-1231
17. Boyko OB, Cory DA, Cohen MD, Provisor A, Mirkin D, DeRosa GP. MR imaging of osteogenic and Ewing's sarcoma. AJR Am J Roentgenol. 1987 Feb; 148(2):317-22.
18. Jelinek, J. S., Kransdorf, M. J., & Shmookler, B. M. (1995). MRI of benign bone tumors. Radiologic Clinics of North America, 33(4), 893-915.
19. Wang T, Wu X, Cui Y, Chu C, Ren G, Li W. Role of apparent diffusion coefficients with diffusion-weighted magnetic resonance imaging in differentiating between benign and malignant bone tumors. World J Surg Oncol 2014; 12: 365. doi: https://doi.org/ 10.1186/1477-7819-12-365
20. Pekcevik Y, Kahya MO, Kaya A. Diffusion-weighted magnetic resonance imaging in the diagnosis of bone tumors: preliminary results. J Clin Imaging Sci 2013; 3: 63Available from. doi: https://doi.org/10. 4103/2156-7514.124094
21. Shimose, S., Sugita, T., Kubo, T., Matsuo, T., Nobuto, H., & Ochi, M. (2008). Differential diagnosis between osteomyelitis and bone tumors. Acta Radiologica, 49(8), 928-933.
22. Yeslawath AND. Study to evaluate the role of MRI in cases of primary malignant bone tumors. IAIM, 2016; 3(3): 87-94.
23. Farooq, A., Zameer, S., Khadim, R., & Manzoor, A. (2021). Diagnostic accuracy of magnetic resonance imaging in diagnosing bone tumors keeping histopathological correlation as gold standard. Pakistan Armed Forces Medical Journal, 71(Suppl-1), S207-12.
24. McCarville MB, Chen JY, Coleman JL, Li Y, Li X, Adderson EE, Neel MD, Gold RE, Kaufman RA. Distinguishing Osteomyelitis From Ewing Sarcoma on Radiography and MRI. AJR Am J Roentgenol. 2015 Sep;205(3):640-50; quiz 651. doi: 10.2214/AJR.15.14341. PMID: 26295653; PMCID: PMC5744678.
25. Bhuyan MH, Bhuyan RK. How accurate is MRI in prediction of musculoskeletal tumors - A prospective evaluation. Int J Business Res 2015; 6(12): 942-46
26. Murphey, M. D., Choi, J. J., Kransdorf, M. J., Flemming, D. J., & Gannon, F. H. (2000). Imaging of osteochondroma: variants and complications with radiologic-pathologic correlation. Radiographics, 20(5), 1407-1434.